SUPPLEMENTAL FIGURES

Figure S1, related to Figure 1. Irinotecan Activation and Metabolism Schematic. Irinotecan (also known as CPT-11) is a prodrug that is activated by esterases to SN-38, which targets topoisomerase I-DNA complexes. SN-38 is glucuronidated by UDP-glucuronosyltransferases to SN-38-G, which is sent to the GI. In the intestines, SN-38-G can be reactivated to SN-38 by β-glucuronidase enzymes expressed by bacterial symbiotes. Reactivated SN-38 can significantly harm the GI epithelium, leading to dose-limiting diarrhea. Inhibitors of microbial β-glucuronidases are expected to block the reactivation of SN-38-G to SN-38, and to reduce GI toxicity.

Figure S1

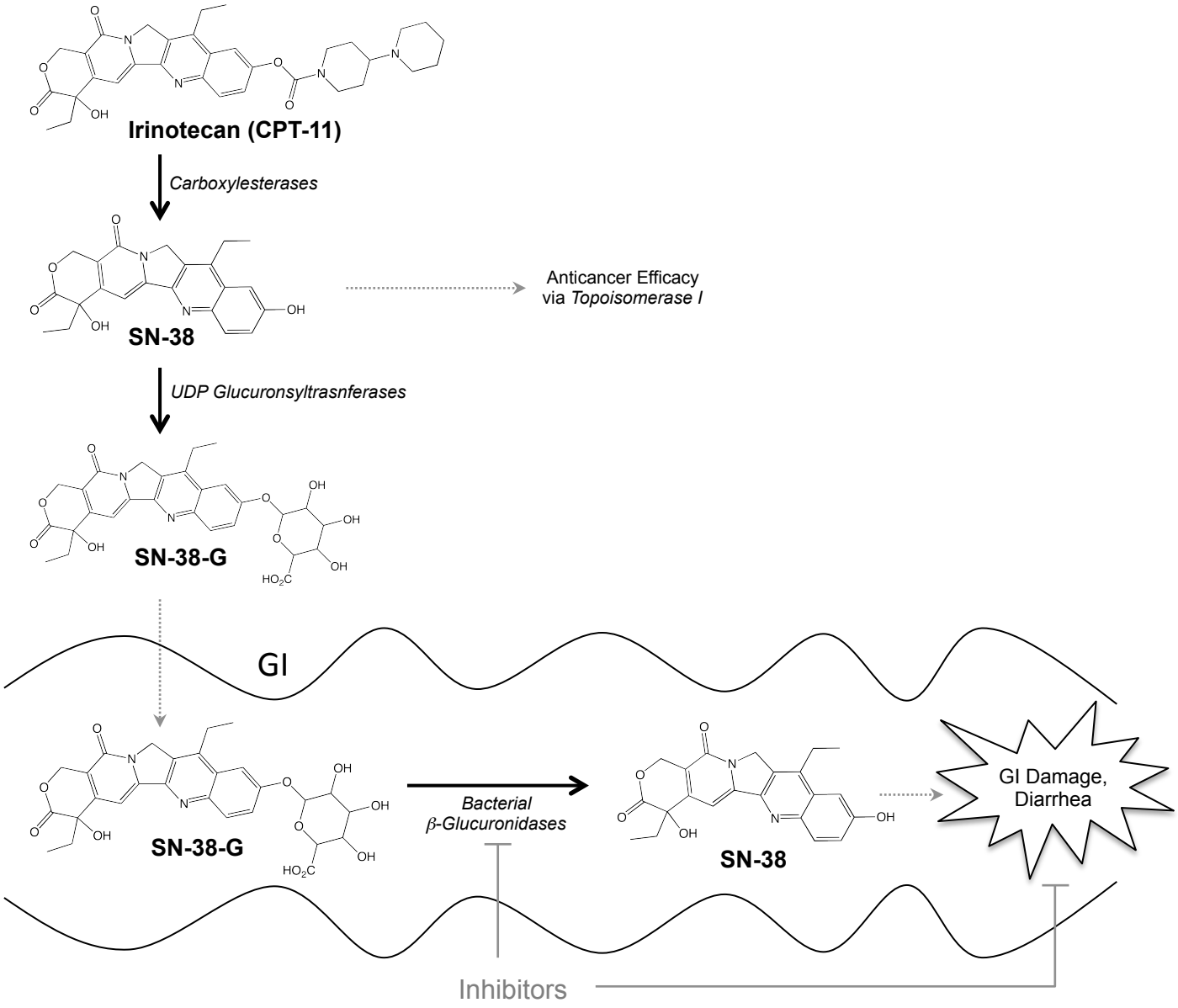
Irinotecan (CPT-11)
Carboxylesterases
SN-38
Anticancer Efficacy
via Topoisomerase I
UDP Glucuronsyltrasnferases
SN-38-G
GI
SN-38-G
Bacterial
β-Glucuronidases
SN-38
GI Damage,
Diarrhea
Inhibitors

Figure S2, related to Figure 2. A. Overlay of *Clostridium perfringens* β-glucuronidase (yellow) and *Escherichia coli* β-glucuronidase (red) in complex with Inhibitor 2 (orange) showing the structural flexibility of this region. **B**. Overlay of *Streptococcus agalactiae* β-glucuronidase I222 (teal) or $P2_12_12$ (magenta) and *Escherichia coli* β-glucuronidase (red) in complex with Inhibitor 2 (orange).

Figure S2

A

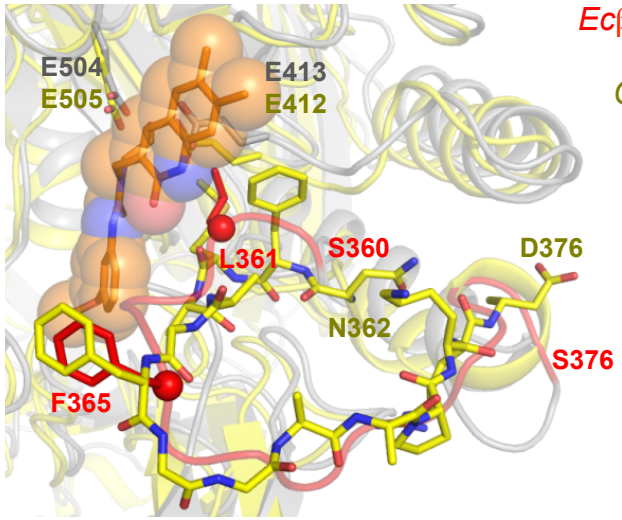

*Ec*βG-Inh2
vs.
*Cp*βG

B

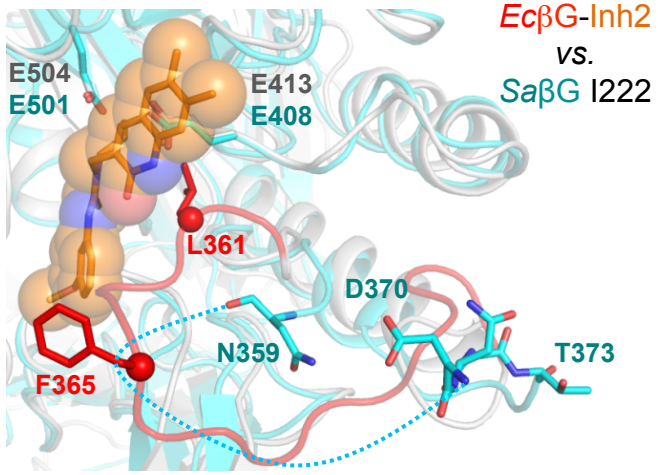

*Ec*βG-Inh2
vs.
*Sa*βG I222

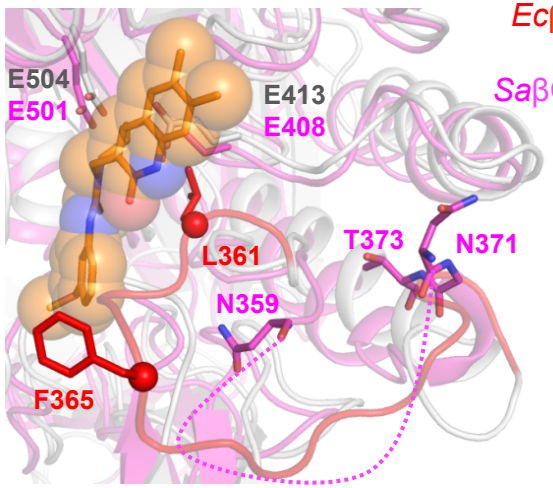

*Ec*βG-Inh2
vs.
*Sa*βG $P2_12_12$

Figure S3 related to Figure 3. Bacterial β-glucuronidase inhibitors 1-8. See Table S2 for Ki data against *Cp*GUS, *Sa*GUS, and *Ec*GUS. Inhibitor 1-4 first characterized in Wallace *et al.* (Wallace et al., 2010). Inhibitors 5-8 first characterized in Roberts *et al.* (Roberts et al., 2013).

Figure S3

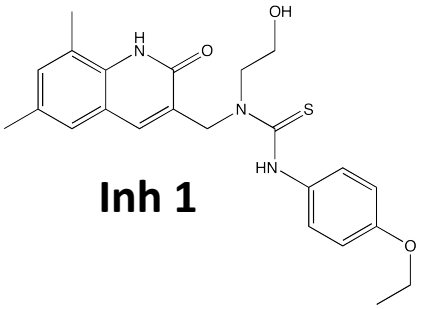

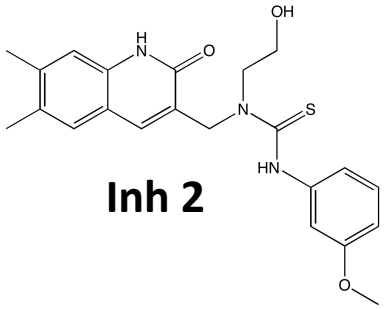

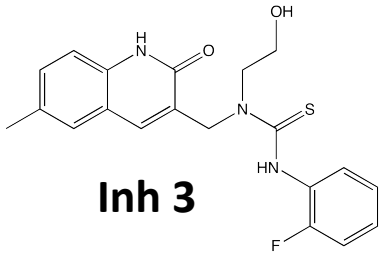

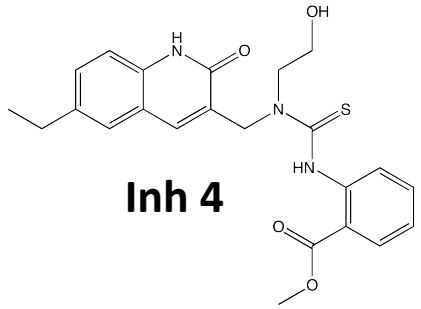

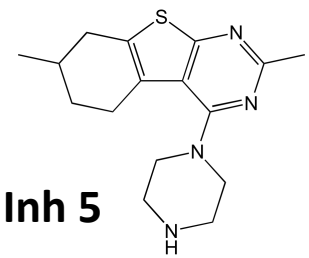

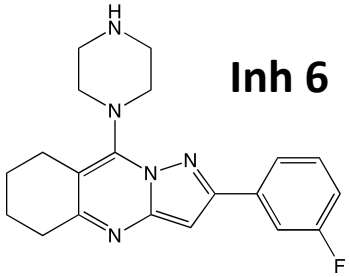

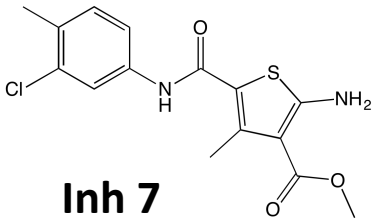

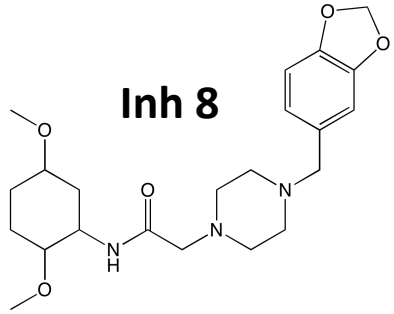

Figure S4 related to Figure 2. Oligomer States of GUS Enzymes. While both *E. coli* β-glucuronidase (*Ec*GUS) and *Bacteroides fragilis* β-glucuronidase (*Bf*GUS) form crystallographic tetramers, they are distinct from one another. As such, *Ec*GUS creates a binding site for inhibitor associate that *Bf*GUS cannot form (see Figure 2D).

Figure S4

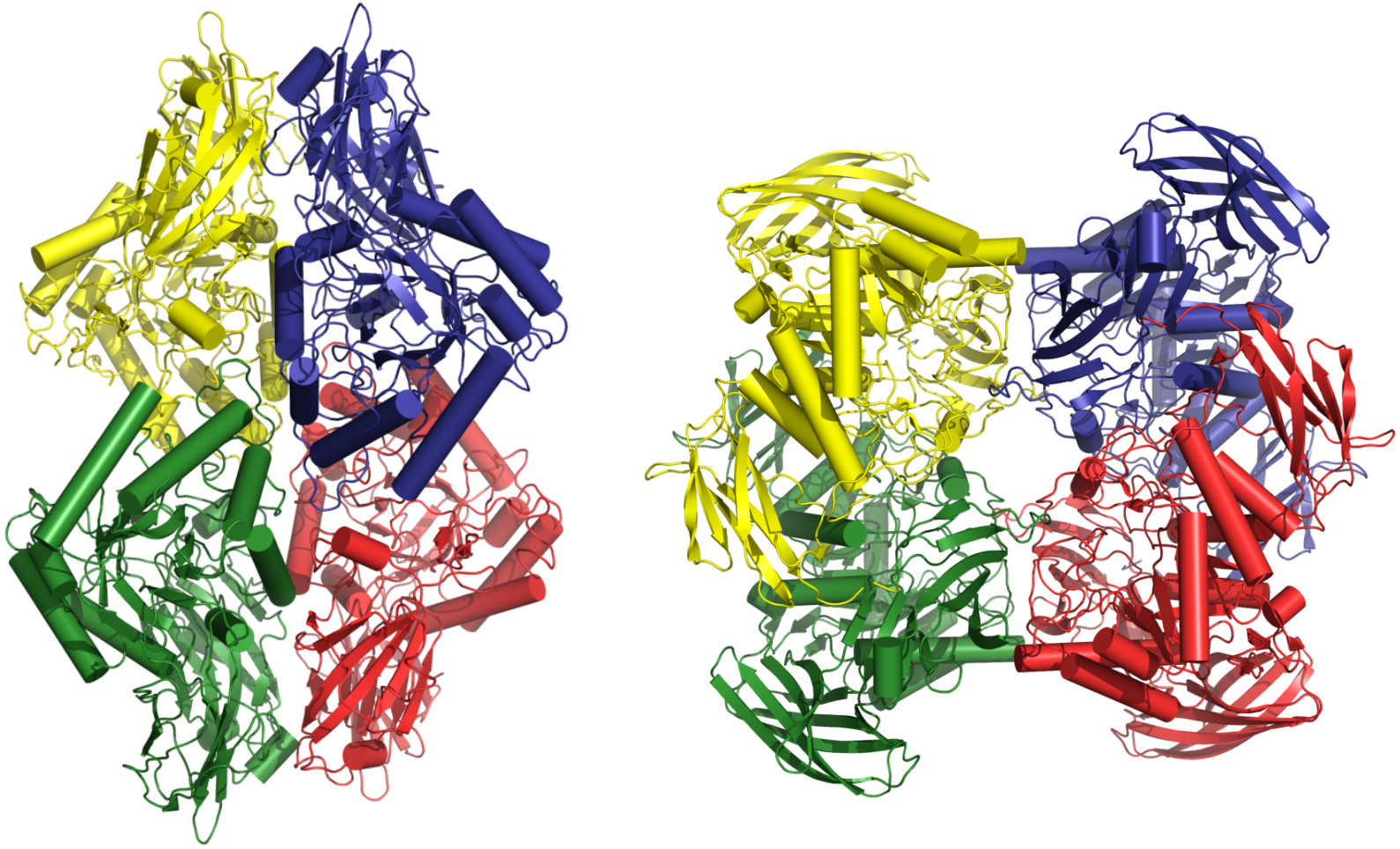

*Ec*GUS

*Bf*GUS

Figure S5 related to Figure 3. Synthetic scheme for the creation of Inhibitors R1 and R3.

Figure S5

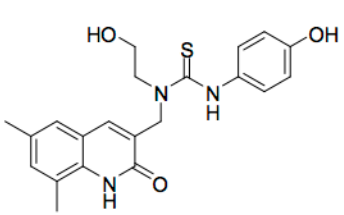

Inhibitor R1

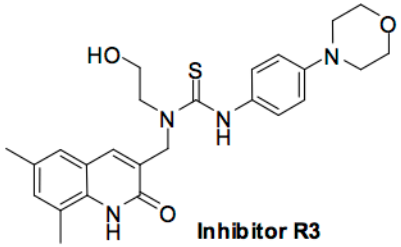

Inhibitor R3

Synthetic route:

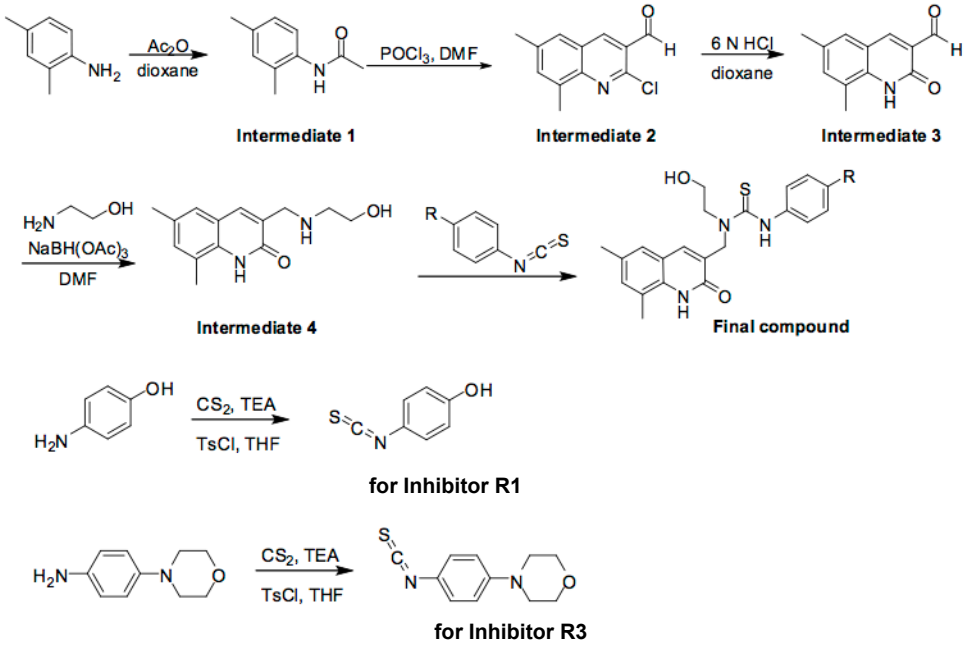

Figure S6 related to Figure 3. A., B. NMR spectra of Inhibitors R1 and R3, respectively. **C., D.** Mass spectrometry analysis of Inhibitors R1 and R3.

Figure S6

A

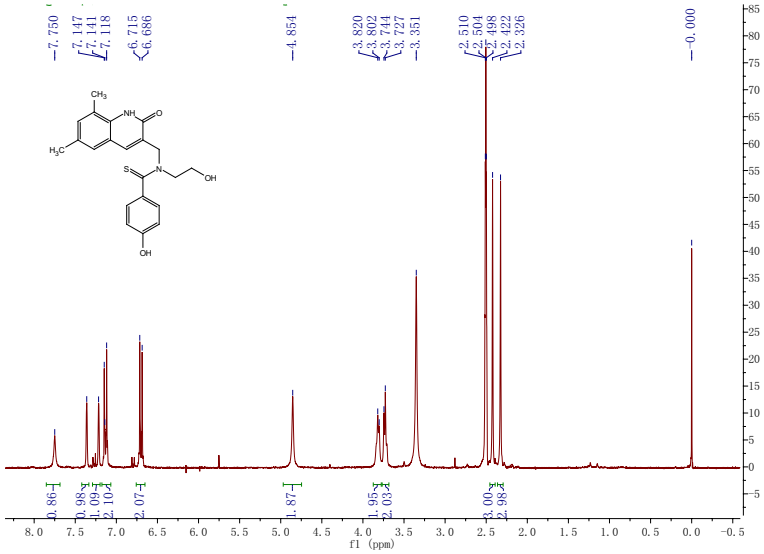

B

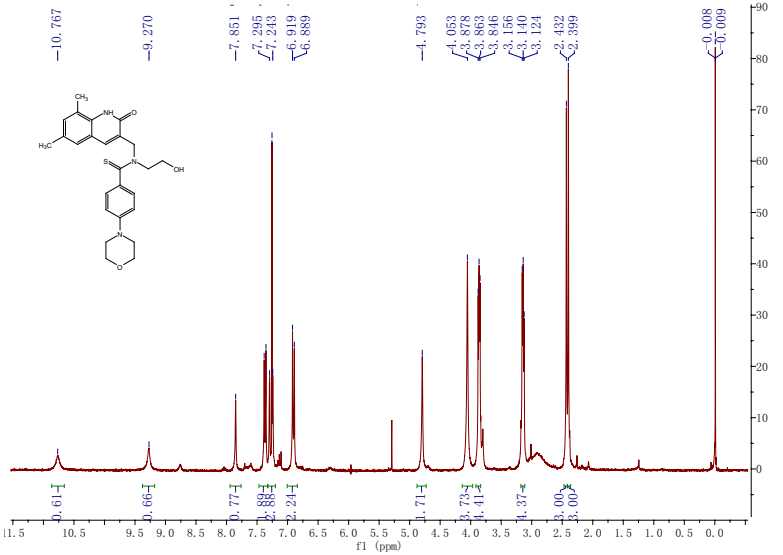

C

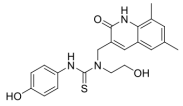

Chemical Formula: $C_{21}H_{23}N_3O_3S$
Exact Mass: 397.146
Molecular Weight: 397.491

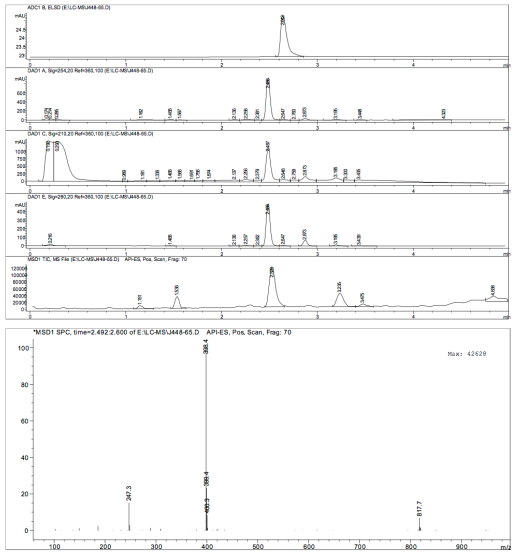

D

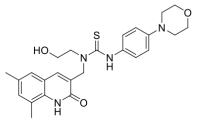

Chemical Formula: $C_{25}H_{30}N_4O_3S$
Exact Mass: 466.204
Molecular Weight: 466.596

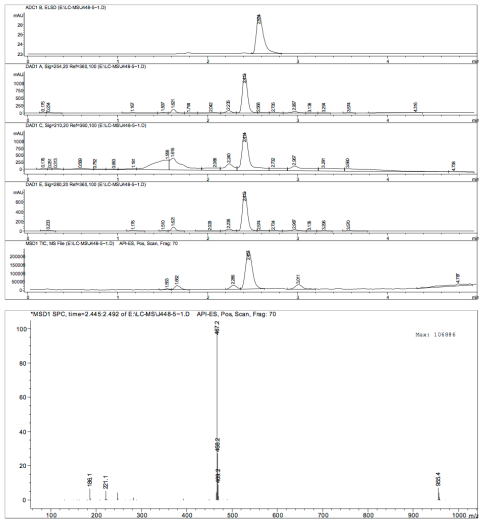

Figure S7 related to Figure 2. Phylogenetic Analysis and Loop Status of Taxonomically Diverse β-Glucuronidases. Phylum-level taxonomy is indicated by branch color. The tree is rooted using the *E. coli* β-galactosidase (BGAL_ECOLI) sequence as an outgroup. Loop-containing sequences, which we term L-GUS, are indicated with salmon colored bars, and no-loop sequences (NL-GUS) are indicated with blue colored bars. Black circles indicate bootstrap values of 60/100 or better. The GUS enzymes considered here in structural detail are indicated.

Figure S7

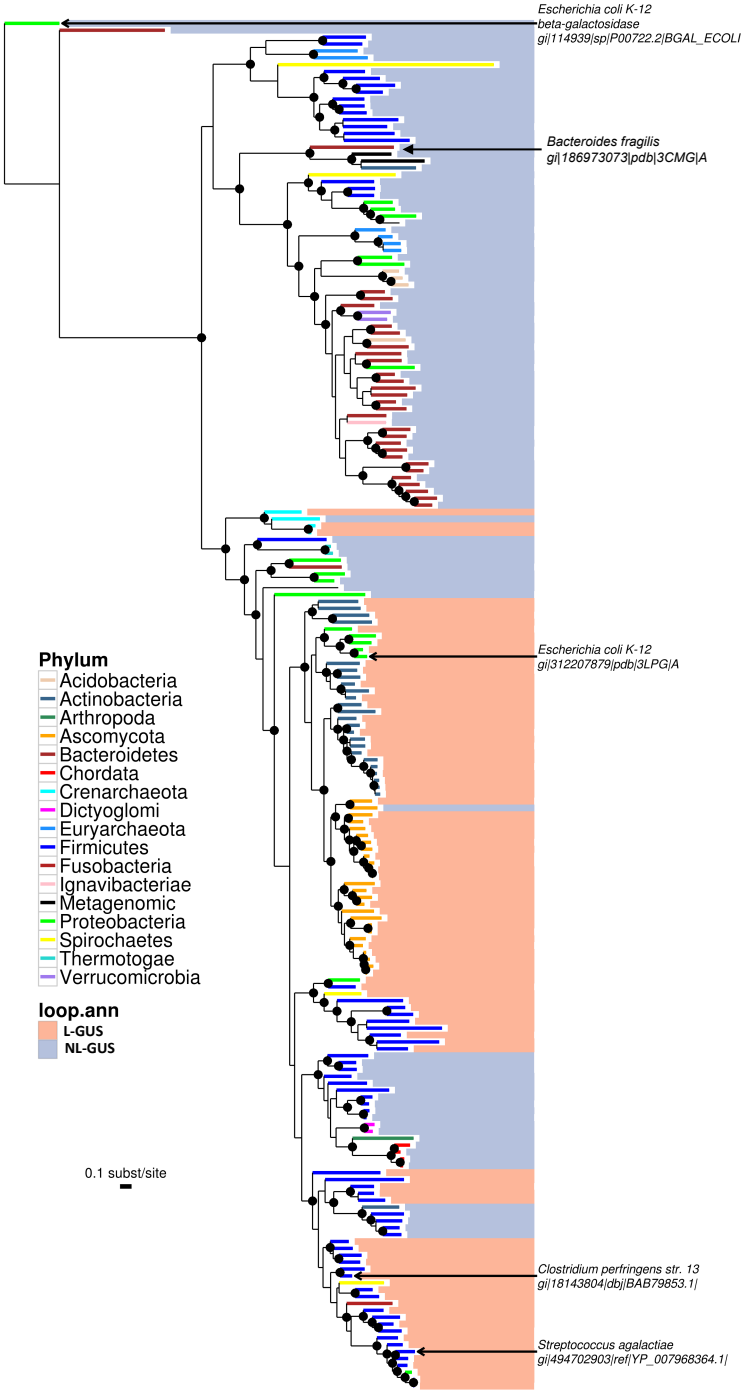
Escherichia coli K-12
beta-galactosidase
gi|114939|sp|P00722.2|BGAL_ECOLI
Bacteroides fragilis
gi|186973073|pdb|3CMG|A
Escherichia coli K-12
gi|312207879|pdb|3LPG|A
Clostridium perfringens str. 13
gi|18143804|dbj|BAB79853.1|
Streptococcus agalactiae
gi|494702903|ref|YP_007968364.1|
Phylum
Acidobacteria
Actinobacteria
Arthropoda
Ascomycota
Bacteroidetes
Chordata
Crenarchaeota
Dictyoglomi
Euryarchaeota
Firmicutes
Fusobacteria
Ignavibacteriae
Metagenomic
Proteobacteria
Spirochaetes
Thermotogae
Verrucomicrobia
loop.ann
L-GUS
NL-GUS
0.1 subst/site

SUPPLEMENTAL TABLES

Table S1, related to Figure 1. Crystallographic Statistics

Structures of *Clostridium perfringens* (*Cp*GUS), *Streptococcus agalactiae* (*Sa*GUS), *Escherichia coli* (*Ec*GUS) β-glucuronidases in complex with Inhibitor R1. APS GM/CA-CAT is The National Institute of General Medical Sciences and National Cancer Institute Structural Biology Facility at the Advance Photon Source; AU is asymmetric unit; R.M.S. is root mean square.

Table S1

Data Collection				
Structure (RCSB ID)	*Cp*GUS – MBP (4JKM)	*Sa*GUS (4JKK)	*Sa*GUS (4JKL)	*Ec*GUS – InhR1 (5CZK)
X-ray source	APS GM/CA-CAT 23-ID			
Space group	$C222_1$	I222	$P2_12_12$	C2
Unit cell: a, b, c (Å); α=β=γ=90° unless noted	71, 293, 240	69, 84, 200	85, 199, 76	169, 76, 126; β=125
Resolution (Å) (highest shell)	50.0-2.26 (2.34-2.26)	50.0-2.60 (2.64-2.60)	50.0-2.30 (2.38-2.30)	42 -2.39 (2.48 -2.39)
I/σ	12.0 (2.0)	19.8 (7.2)	14.3 (3.2)	12.28 (2.3)
Completeness (%)	99.6 (96.1)	99.0 (90.3)	98.1 (88.6)	99.0 (91.1)
Redundancy	7.4 (6.9)	6.6 (6.4)	12.4 (7.2)	5.1 (5.1)
Refinement				
Resolution (Å)	50-2.3	50-2.6	50-2.3	42-2.4
No. of unique reflections	117082	17216	57496	51255
R_{work}	0.219	0.146	0.174	0.196
R_{free}	0.248	0.215	0.226	0.246
Molecules per asymmetric unit (AU)	2 *Cp*GUS-MBP	1 *Sa*GUS	2 *Sa*GUS	2 *Ec*GUS – InhR1
No. of amino acids per AU	1807	588	1174	1201
No. of waters per AU	513	295	774	407
R.M.S. deviations				
Bond lengths (Å)	0.004	0.015	0.002	0.01
Bond angles (°)	0.940	1.44	0.730	1.32
Ramachandran (%)				
Favored	94	96	96	94
Allowed	5.3	3.7	4	5.4
Outliers	0.7	0.3	0	0.6

Table S2, related to Table 1. *In vitro* β-Glucuronidase Inhibition, K_i (μM)

Enzyme inhibition properties of small molecule inhibitors against representative β-glucuronidase enzymes from the mammalian microbiota. Grey data from (Roberts et al., 2013; Wallace et al., 2010). N.I.: no inhibition. Data are presented as the average over > 3 experiments ± SEM for *Escherichia coli* (*Ec*GUS), *Clostridium perfringens* (*Cp*GUS), *Streptococcus agalactiae* (*Sa*GUS), and *Bacteroides fragilis* (*Bf*GUS) β-glucuronidases.

Table S2

Inhibitor	*Cp*GUS	*Sa*GUS	*Ec*GUS	*Bf*GUS
1	0.97 ± 0.1	1.4 ± 0.4	0.16 ± 0.01	*ni*
R1	*ni*	*ni*	1.9 ± 0.5	*ni*
R3	*ni*	*ni*	0.61 ± 0.2	*ni*
2	1.1 ± 0.5	3.0 ± 1	0.21 ± 0.03	*ni*
3	7.8 ± 0.9	11 ± 3	0.68 ± 0.08	*ni*
4	24 ± 3	36 ± 5	1.4 ± 0.2	*ni*
5	0.54 ± 0.2	0.81 ± 0.2	0.22 ± 0.04	*ni*
6	6.1 ± 2	2.8 ± 0.3	0.67 ± 0.03	*ni*
7	*ni*	*ni*	1.9 ± 0.02	*ni*
8	*ni*	*ni*	0.96 ± 0.03	*ni*

Table S3. Cell-based assays for inhibitor efficacy against *E. coli* β-glucuronidase, related to Table 1. Data are presented as the average over > 3 experiments ± SEM.

Table S3

Inhibitor	EC_{50} (μM)
R1	4.5 ± 0.7
R3	3.1 ± 0.1

Table S4, related to Figure 5. **Pharmacokinetic data for CPT-11 and its key metabolites SN-38 and SN-38G.** Mice (N=3) received CPT-11 without (**A**) or with (**B**) Inhibitor 1 (Inh1). T_{max} is the time at which maximal analyte was observed (either CPT-11, SN-38 or SN-38G). $T_{1/2}$ is the half-life of analyte presence in serum; for SN-38 alone or with Inh1, no error on 0.08 hours was observed. C_{max} is the maximum analyte concentration observed, and AUC is the area under the curve for each analyte.

Table S4

	T_{max} (hr)	$T_{1/2}$ (hr)	C_{max} (ng/mL)	AUC (ng/mL*hr)
CPT-11	0.42 ± 0.1	2.6 ± 0.2	56,000 ± 8,000	150,000 ± 20,000
CPT-11 + Inh1	0.42 ± 0.1	2.3 ± 0.3	88,000 ± 10,000	190,000 ± 30,000
SN-38	0.08	4.6 ± 0.2	1,300 ± 100	2,000 ± 40
SN-38 + Inh1	0.08	5.6 ± 0.6	1,300 ± 200	1,800 ± 100
SN-38-G	0.42 ± 0.1	4.2 ± 0.3	540 ± 50	2,800 ± 500
SN-38-G + Inh1	0.42 ± 0.1	3.9 ± 0.6	740 ± 100	3,100 ± 600

EXPERIMENTAL PROCEDURES

Beta-Glucuronidase Cloning

Genomic DNA was derived from *Streptococcus agalactiae* 2603V/R (ATCC #BAA-611D-5), and was graciously provided by Dr. Bruce McClane (University of Pittsburgh School of Medicine) for *Clostridium perfringens* str. 13. To clone the β-glucuronidase gene from each species, the following primers were used for PCR amplification: *Streptococcus agalactiae*, forward, 5'-TACTTCCAATCCAATGCGATGTTATATCCATTATTGAC-3', reverse, 5'-TTATCCACTTCCAATGCGCTACTATTTTACACTATTTTTTTTATTATG-3'; *Clostridium perfringens*, forward, 5'-TACTTCCAATCCAATGCGATGTTATATCCAATAATTACAGAATCAAG-3', reverse, 5'-TTATCCACTTCCAATGCGCTATTATTTTTTGTATCCAAATTCCG-3'. The PCR amplified β-glucuronidase genes were inserted into pLIC-His (*Streptococcus agalactiae*) and pLIC-MBP (*Clostridium perfringens*) ligation independent cloning (LIC) vectors. The pLIC-His vector contains an N-terminal 6x-Histidine tag, and the pLIC-MBP plasmid incorporates an N-terminal MBP-fusion and 6x-Histidine tag.

Protein Expression and Purification

BL21-DE3 AI competent cells (Invitrogen) were transformed with plasmids containing full-length *Streptococcus agalactiae* β-glucuronidase (*Sa*GUS) and *Clostridium perfringens* β-glucuronidase (*Cp*GUS) for enzyme expression. Cells were grown in the presence of ampicillin in LB medium with vigorous shaking at 37 °C until an OD_{600} of 0.6 was attained. Protein expression was induced with the addition of 100 uM arabinose and 0.3 mM isopropyl-1-thio-D-galactopyranoside (IPTG) and further incubated overnight at 18 °C. Cells were collected by centrifugation at 4500xg for 20 min at 4 °C in a Sorvall (model RC-3B) swinging bucket centrifuge. Cell pellets were resuspended in Buffer A

(25 mM HEPES, pH 7.4, 50 mM Imidazole, 500 mM NaCl, 5% Glycerol, 0.5 mM TCEP) and a Roche complete-EDTA free protease inhibitor tablet per 50 mL buffer. Resuspended cells were sonicated and centrifuged at 14,500xg for 60 min in a Sorvall (model RC-5B) centrifuge to clarify the lysate. The lysate was flowed over a Ni-NTA HP column (GE Healthcare), loaded onto the Äktaxpress FPLC system (Amersham Biosciences) and washed with Buffer A. Protein was eluted with Buffer B (25 mM HEPES, pH 7.4, 500 mM Imidazole, 500 mM NaCl, 5% Glycerol, 0.5 mM TCEP). Purity of eluted fractions was assessed by SDS-PAGE. Purest fractions were combined and passed over a HiLoad™ 16/60 Superdex™ 200 gel filtration column. The protein was eluted into 20 mM HEPES, pH 7.4, 100 mM NaCl, and 0.5 mM TCEP for crystallization and activity assays. One and a half milliliter fractions were collected based on highest ultraviolet absorbance at 280 nm. Fractions were analyzed by SDS-PAGE (which indicated >95% purity), combined, and concentrated to 10 mg/mL for long-term storage at -80 °C. Full-length *E. coli* β-glucuronidase (*Ec*GUS) was expressed and purified as previously described (Wallace et al., 2010). The *B. fragilis* β-glucuronidase associated with RCSB code 3CMG was overexpressed in *E. coli* as a C-terminal histidine-tagged protein, and purified as described using Ni-affinity and sizing column chromatography. *Ec*GUS and *Bf*GUS samples (1 mg/mL) were examined by multiangle light scattering for oligomerization state in vitro using a Wyatt DAWN HELEOS II light scattering instrument interfaced to an Agilent FPLC System. *Ec*GUS eluted as two peaks, one with mass fraction 99.2% and the other with a fraction of 0.8%. The larger peak showed a molecular mass of 278 kDa, close to the calculated molecular weight of an *Ec*GUS tetramer of 288 kDa. *Bf*GUS eluted as a single peak with molecular mass corresponding to 304 kDa, close to its predicted tetramer molecular weight of 336 kDa.

Crystallization, Data Collection, and Structure Determination

His-*Sa*GUS and MBP-*Cp*GUS were initially screened for crystallization conditions using the PEGs I suite from Qiagen. His-*Sa*GUS crystals were optimized for quality in 0.1-0.3 M potassium thiocyanate and 20-28% PEG 3350 at 16 °C. Crystals of MBP-*Cp*GUS were grown at 16 °C in 0.1 M MES, pH 6.0-6.5, 28-36% PEG 400. Crystals were flash frozen in liquid nitrogen in preparation for x-ray data collection. Diffraction data was collected on the 23-ID beam line at GM/CA-CAT (Advanced Photon Source, Argonne National Laboratory). Two datasets were collected for *Sa*GUS, and were indexed and scaled using HKL2000 (Otwinowski et al., 1997). Data reduction for the *Cp*GUS was performed by XDS (Kabsch, 2010).

The *Sa*GUS crystals yielded two forms, one that scaled in the space group I222 and yielded diffraction data to 2.6 Å resolution, and the other in $P2_12_12$ that produced diffraction data to 2.3 Å resolution. *Cp*GUS crystals diffracted to 2.3 Å resolution and were scaled in $C222_1$. All three structures were solved by molecular replacement using Phaser (Grosse-Kunstleve and Adams, 2007) with the *E. coli* β-glucuronidase structure as a model (PDB ID 3K46). Initial models were manually adjusted using Coot (Emsley and Cowtan, 2004) and $2F_o$-F_c and F_o-F_c electron density maps. The structures were refined using simulated annealing, torsion angle, and B-factor refinement using Phenix (Adams et al., 2002). Model quality during refinement was monitored using both the crystallographic R and cross-validating R-free statistics (Brünger, 1997). Data collection and refinement statistics for the two *Sa*GUS and one *Cp*GUS crystal structures are presented in Table S1.

The *E. coli* β-glucuronidase (*Ec*GUS)-R1 complex crystals were obtained as first described in Wallace *et al.* (Wallace et al., 2010) with modifications for co-crystallization as described in Roberts *et al.* (Roberts et al., 2013). Briefly, 2 mg/ml *Ec*GUS protein with

30- to 100-fold molar excess Inhibitor R1 yielded crystals in 17% polyethylene glycol 3350 (w/v), 250 mM magnesium acetate, and 0.02% sodium azide (w/v) at 16 °C. Crystals were cryoprotected with perfluoropolyether vacuum pump oil (Sigma-Aldrich) and flash-cooled in liquid nitrogen. Diffraction data were obtained and processed, and the structure was determined and refined as described above for *Cp*GUS and *Sa*GUS.

Enzyme Assays

Inhibitors 1-8 (Figure S5) were purchased from Asinex, Inc. (Winston-Salem, NC), while Inhibitors R1 and R3 were synthesized in-house according to Figure S7 and validated by NMR and mass spectrometry, as shown in Figure S8. Each compound started as solid powder and was resuspended in 100% dimethyl sulfoxide (DMSO) at 25 mM prior to dilution for use. Assays were performed using the His-*Sa*GUS, MBP-*Cp*GUS, and His-*Ec*GUS enzymes. Kinetic assays used *p*-nitrophenyl glucuronide (PNPG) as the absorbance substrate. Reactions were conducted in 96-well, clear bottom assay plates (Costar, Tewksbury, MA) at 37 °C in 50 uL total volume. The reaction consisted of 10 uL assay buffer (100 mM HEPES, 250 mM NaCl, pH 7.4), 10 uL enzyme, and 30 uL of substrate. The reaction was performed at 37 °C and product formation was measured using a PHERAstar *Plus* microplate reader (BMG Labtech, Ortenberg, Germany). Initial velocities were determined for multiple substrate and enzyme concentrations and Michaelis-Menten kinetics used to calculate K_M, k_{cat}, and catalytic efficiency.

Inhibition assays were performed using the same enzymes to assess the efficiency of Inhibitors 1-8, R1, and R3 to disrupt enzymatic activity from various bacterial species. Reactions were conducted similarly to the kinetic assays but the reaction consisted of 10 uL assay buffer, 5 uL inhibitor solution, 5 uL of 10 nM enzyme, and 30 uL of substrate. The reaction was incubated at 37 °C for 6 hours to allow the reaction to reach

equilibrium and then quenched with 100 uL of 0.2 M sodium carbonate. Initial velocities were determined for multiple substrate and inhibitor concentrations and the inhibition constant values, K_i, were calculated for Inhibitors 1-8, R1, and R3 (Table S2) using SigmaPlot 11.0. Cell-based assays to calculate EC_{50} were performed as described (Roberts et al., 2013; Wallace et al., 2010). Briefly, HB101 *E. coli* cells containing the pET28a vector with the β-glucuronidase gene were grown to an OD_{600} of 0.6. The reaction proceeded similarly to the *in vitro* assay described above but the reaction mixture consisted of 39 µL of cells, 10 µL substrate (1 mM PNPG) and 1 µL inhibitor (varying concentrations). HPLC assays of SN-38-G (Santa Cruz Biotech) conversion to SN-38 (Santa Cruz Biotech) were conducted as described (Wallace et al., 2010).

Identification of Diverse β-Glucuronidase Sequences

Enzyme Commission identifier 3.2.1.31 was employed to locate cultured β-glucuronidase sequences in the carbohydrate active enzyme (CAZy) resource (Lombard et al., 2014) via the dbCAN database (Yin et al., 2012). Sequences were clustered at 70% identity with USEARCH (Edgar, 2010) to retain a phylogenetically diverse set of β-glucuronidases. Two recently described metagenomic β-glucuronidases from the human gut were also included (Gloux et al., 2011). This base set of β-glucuronidases, primarily from bacteria, was next used to identify additional representatives from the less-represented archaeal and fungal sequences as follows: β-glucuronidases were compared to only archaeal and fungal sequences from the Genbank database (Benson et al., 2013) based on taxonomy identifier using BLASTP (Altschul et al., 1990) with an e-value cutoff of e^{-50} to retain only strong hits. Resulting sequences were then clustered at 90% identity using USEARCH to remove highly similar sequences.

β-Glucuronidase Phylogenetic Tree Construction

The β-glucuronidase sequences collected as described above were aligned using MUSCLE (Edgar, 2004). The alignment was then trimmed to require that 80% of each column was covered; this step prevents retaining regions of the protein that are only present in a small number of sequences. Trees were reconstructed with PhyML (Guindon et al., 2010) using one category of substitution rate, the JTT model of amino acid substitution, the proportion of invariable sites was fixed, and 100 bootstrap replicates were created to determine branch support. The closely related but functionally distinct β-galactosidase gene from *Escherichia coli* was used as an outgroup to root the tree; the β-galactosidase gene 3DEC was included as an example of a potential β-galactosidase that was instead annotated as a β-glucuronidase. The tree was plotted with the R packages "phyloseq", "ape", and "ggplot2" (McMurdie and Holmes, 2013; Paradis et al., 2004; Wickham, 2009).

CPT-11 and Inhibitor Studies in Mice

Alleviation of CPT-11-induced toxicity studies were performed as described previously (Roberts et al., 2013). Inhibitor R1 and R3 pharmacokinetic analyses were performed identically to that described previously (LoGuidice et al., 2012). CPT-11, SN-38 and SN-38-G pharmacokinetic analysis was performed as follows: CPT-11 was administered at 50 mg/kg i.p. x 1 with or without 20 μg of Inhibitor 1 per day (oral gavage of 10 μg twice daily for 3 days prior to CPT-11 administration and once at CPT-11 administration) in Balb/cJ wild-type mice. Blood samples were obtained in sodium heparin from mice sacrificed at 0 min, 5 min, 15 min, 30 min, 1 h, 3 h, 6 h, and 24 h after CPT-11 administration (n = 3 per timepoint). Plasma was isolated and stored at -80°C until analysis. Samples were prepared via protein precipitation in acetonitrile with CPT (camptothecin; Sigma-Aldrich, St. Louis, MO) as an internal standard. Analytes were separated using a Shimadzu LC-20 HPLC equipped with a Waters XBridge C18 column

(2.5 µm, 2.1 x 50 mm). Separation occurred at 60°C in an acidified acetonitrile gradient at 0.6 mL/min over a total of 3.0 min. Quantitative analysis was performed by a Thermo Exactive Orbitrap mass spectrometer equipped with a heated ESI source and operating in positive mode with enhanced resolution and optimized for high dynamic range. The full mass range was scanned from 200 – 600 m/z for analyte detection. Analytical ranges were 1 – 1000 ng/mL for CPT-11, 1 – 3000 ng/mL for SN-38, and 1 – 5000 ng/mL for SN-38G. Pharmacokinetic parameters were determined with Phoenix v. 6.3 (Pharsight, Mountain View, CA) using non-compartmental analysis.

SUPPLEMENTAL REFERENCES

Altschul, S.F., Gish, W., Miller, W., and Myers, E.W. (1990). Basic local alignment search tool. Journal of Molecular Biology *215*, 403–410.

Adams, P.D., Grosse-Kunstleve, R.W., and Hung, L.W. (2002). PHENIX: building new software for automated crystallographic structure determination. Acta Crystallographica *58*, 1948-1954.

Benson, D.A., Cavanaugh, M., Clark, K., Karsch-Mizrachi, I., Lipman, D.J., Ostell, J., and Sayers, E.W. (2013). GenBank. Nucleic Acids Res. *41*, D36–D42.

Brünger, A.T. (1997). Free R value: cross-validation in crystallography. Meth. Enzymol. *277*, 366–396.

Edgar, R.C. (2004). MUSCLE: multiple sequence alignment with high accuracy and high throughput. Nucleic Acids Res. *32*, 1792–1797.

Edgar, R.C. (2010). Search and clustering orders of magnitude faster than BLAST. J Gerontol *26*, 2460–2461.

Emsley, P., and Cowtan, K. (2004). Coot: model-building tools for molecular graphics. Acta Crystallographica Section D. *D60*, 2126-2132.

Gloux, K., Berteau, O., Oumami, El, H., Béguet, F., Leclerc, M., and Doré, J. (2011). A metagenomic β-glucuronidase uncovers a core adaptive function of the human intestinal microbiome. Proc. Natl. Acad. Sci. U.S.a. *108 Suppl 1*, 4539–4546.

Grosse-Kunstleve, R.W., and Adams, P.D. (2007). Phaser crystallographic software. J. Applied Crystallography. *40*, 658-674.

Guindon, S., Dufayard, J.-F., Lefort, V., Anisimova, M., Hordijk, W., and Gascuel, O. (2010). New algorithms and methods to estimate maximum-likelihood phylogenies: assessing the performance of PhyML 3.0. Syst. Biol. *59*, 307–321.

Kabsch, W. (2010). Xds. Acta Crystallographica Section D. *D66*, 125-132.

LoGuidice, A., Wallace, B.D., Bendel, L., Redinbo, M.R., and Boelsterli, U.A. (2012). Pharmacologic targeting of bacterial β-glucuronidase alleviates nonsteroidal anti-inflammatory drug-induced enteropathy in mice. J. Pharmacol. Exp. Ther. *341*, 447–454.

Lombard, V., Ramulu, H.G., Drula, E., Coutinho, P.M., and Henrissat, B. (2014). The carbohydrate-active enzymes database (CAZy) in 2013. Nucleic Acids Res. *42*, D490–D495.

McMurdie, P.J., and Holmes, S. (2013). phyloseq: an R package for reproducible interactive analysis and graphics of microbiome census data. PLoS ONE *8*, e61217–e61217.

Otwinowski, Z., and Minor,W. Processing of X-ray Diffraction Data Collected in Oscillation Mode, *Methods in Enzymology*, Volume 276: Macromolecular

Crystallography, part A, p.307-326, 1997,C.W. Carter, Jr. & R. M. Sweet, Eds., Academic Press (New York).

Paradis, E., Claude, J., and Strimmer, K. (2004). APE: Analyses of Phylogenetics and Evolution in R language. Bioinformatics *20*, 289–290.

Roberts, A.B., Wallace, B.D., Venkatesh, M.K., Mani, S., and Redinbo, M.R. (2013). Molecular Insights into Microbial β-Glucuronidase Inhibition to Abrogate CPT-11 Toxicity. Mol. Pharmacol. *84*, 208–217.

Wallace, B.D., Wang, H., Lane, K.T., Scott, J.E., Orans, J., Koo, J.S., Venkatesh, M., Jobin, C., Yeh, L.-A., Mani, S., et al. (2010). Alleviating cancer drug toxicity by inhibiting a bacterial enzyme. Science *330*, 831–835.

Wickham, H. (2009). ggplot2: elegant graphics for data analysis.

Yin, Y., Mao, X., Yang, J., Chen, X., Mao, F., and Xu, Y. (2012). dbCAN: a web resource for automated carbohydrate-active enzyme annotation. Nucleic Acids Res. *40*, W445–W451.